Nonlinear wave propagation in acoustic metamaterials with bilinear nonlinearity

Shiqi Liang(梁诗琪)[1], Jiehui Liu(刘杰惠)[1], Yun Lai(赖耘)[1,†], and Xiaozhou Liu(刘晓宙)[1,2,‡]

[1] *Key Laboratory of Modern Acoustics, Institute of Acoustics and School of Physics, Collaborative Innovation Center of Advanced Microstructures, Nanjing University, Nanjing* 210093, *China*
[2] *State Key Laboratory of Acoustics, Institute of Acoustics, Chinese Academy of Sciences, Beijing* 100190, *China*

(Received 6 August 2022; revised manuscript received 27 September 2022; accepted manuscript online 5 October 2022)

Nonlinear phononic crystals have attracted great interest because of their unique properties absent in linear phononic crystals. However, few researches have considered the bilinear nonlinearity as well as its consequences in acoustic metamaterials. Hence, we introduce bilinear nonlinearity into acoustic metamaterials, and investigate the propagation behaviors of the fundamental and the second harmonic waves in the nonlinear acoustic metamaterials by discretization method, revealing the influence of the system parameters. Furthermore, we investigate the influence of partially periodic nonlinear acoustic metamaterials on the second harmonic wave propagation, and the results suggest that pass-band and band-gap can be transformed into each other under certain conditions. Our findings could be beneficial to the band gap control in nonlinear acoustic metamaterials.

Keywords: bilinear nonlinearity, phononic crystal, band-gap manipulation, nonlinear acoustic metamaterial

PACS: 43.25.+y, 43.25.Ed , 43.35.–c **DOI:** 10.1088/1674-1056/ac9783

1. Introduction

Phononic crystals and metamaterials are acoustic materials or structures with periodic distribution of elastic constant and density. Since the proposal of the seminal concept,[1] a tremendous amount of efforts have devoted to the field of acoustic metamaterials. With the continuous exploration in the past decades, acoustic metamaterials have been found to exhibit interesting exotic properties, such as low-frequency acoustic absorption,[2,3] negative refraction,[4–8] acoustic lens,[9–12] acoustic cloak,[13–17] and so on. These developments indicate that acoustic metamaterials could have practical potential applications in the future.

Besides the development of linear acoustics, researchers have also grown a strong interest in studying the nonlinear properties in acoustic metamaterials. For instance, Cheng *et al.* realized unidirectional acoustic transmission by using phononic crystals and strong acoustic nonlinear media.[18] Wen *et al.* designed a nonlinear acoustic metamaterial based on chaotic band theory, which was able to reduce the vibration of sound waves in an ultra-low and ultra-broad band.[19] Guo *et al.* attained the transformation from fundamental wave to second harmonic wave through a mass-spring system with elastic nonlinearity.[20] Kulkarni *et al.* realized passive direction-bias of acoustic waves using a mass-spring system which introduced local resonance.[21] Grinberg *et al.* investigated the propagation characteristics of elastic waves in phononic crystals with periodically distributed solid–solid rough surface contact interfaces.[22] Golub *et al.* studied the influence of periodic arrays of interface strip-like cracks in layered periodic structures on elastic wave propagation, and found that additional band-gaps would be introduced compared to the case without cracks.[23] Jeon *et al.* used periodic coiling-up space to enhance the down-converted waves.[24] These pioneering researches have enormously deepened our understanding on the consequences of nonlinearity in acoustics.

However, so far, nonlinear metamaterials have still been less studied. Although many researchers started to exploit the opportunities brought by introducing nonlinearity into metamaterials, most of them have focused on investigating the nonlinearity which can be expressed by analytic functions. But in practice, there are many scenarios of nonlinearity that cannot be expressed analytically.

Here, inspired by 'breathing crack model',[25] we assume that there is a kind of nonlinear material unit that can be equivalent to a nonlinear spring. The nonlinear spring we consider is assumed to be bilinear, whose stiffness is dependent on the sign of spring's elongation. We denote this kind nonlinear spring as bilinear nonlinear material unit (BNMU). Different from the classical nonlinear material, the bilinear nonlinear material that we use in this article can generate relatively strong nonlinear even when its length is short, which is beneficial for the miniaturization of devices in practical applications. In this work, we arrange BNMU and isotropy material unit (IMU) periodically to form a one-dimensional (1D) chain of finite waveguides, which is the nonlinear metamaterial, and study the propagation characteristics of fundamental wave and second harmonic wave through this structure. The propagation

†Corresponding author. E-mail: laiyun@nju.edu.cn
‡Corresponding author. E-mail: xzliu@nju.edu.cn

© 2023 Chinese Physical Society and IOP Publishing Ltd

characteristics of fundamental waves are explained by dispersion curves which are obtained by Fourier series expansion of sign function. Additionally, we have also studied the influence of different number cells, in which BNMU and IMU are alternately arranged and inserted in metamaterials on the second harmonic propagation characteristics. By studying the propagation characteristics of acoustic waves in a kind of nonlinear metamaterials with bilinear nonlinear, we reveal the influence of system parameters, as well as the potential application in bandgap manipulation and the transformation between passband and band-gap.

2. Method

2.1. Equations of motion

Figure 1(a) is the schematic diagram of periodic arrangement of nonlinear material unit with bilinear property and isotropic material unit, $P_{\rm inc}$ denotes incident wave, $P_{\rm tr}$ denotes transmitted wave, the red sections represent nonlinear material units with bilinear property, N denotes the number of periodically arranged IMU. Figure 1(b) is the discretization model of periodic arrangement of nonlinear material unit with bilinear property and isotropic material unit, the gray balls represent mass, the red broken lines with arrow represent bilinear nonlinear springs, and the black broken lines without arrow represent linear springs. We assume that BNMU and IMU are arranged periodically, which forms a one-dimensional (1D) chain of finite waveguides, and the length of BNMU is much shorter than which of IMU. For the convenience of study, we assume that the left and right boundaries are half-infinite waveguides, and the IMU between BNMUs is equivalent to the mass-spring system by discretization method, namely two masses, each of which is $\rho aL/2$, connected by a linear spring, whose stiffness is $k_{00}=2\rho ac^2/L$. Among them, ρ is density, a denotes the cross-section area of IMU, L denotes the length of IMU, c is longitudinal wave speed.[22] For simplicity, we set $k_0=2\rho c^2/L$ as the stiffness of IMU with unit cross-section area. Because the length of BNMU is much shorter than IMU, BNMU's mass can be ignored, so that BNMU can be equivalent to a nonlinear spring.

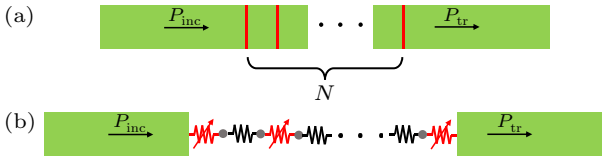


Fig. 1. (a) Schematic diagram of periodic arrangement of nonlinear material unit with bilinear property and isotropic material unit. (b) The discretization model of periodic arrangement of nonlinear material unit with bilinear property and isotropic material unit.

To derive the equations of motion, we analyze the n-th waveguide of the 1D chain. We assume that the stiffness of the nonlinear spring which is the equivalent of the nonlinear material unit with bilinear property with unit cross-section area is

$$k=\begin{cases} k_2, & \Delta\xi>0,\\ k_1, & \text{otherwise}, \end{cases} \tag{1}$$

where ξ denotes displacement, and $k_2<k_1$, then the motion equation of the n-th waveguide can be expressed as

$$\frac{\rho L}{2}\ddot{\xi}_{n,1}+\frac{2\rho c^2}{L}\left(\xi_{n,1}-\xi_{n,2}\right)=-g\left(\xi_{n,1}-\xi_{n-1,2}\right), \tag{2}$$

$$\frac{\rho L}{2}\ddot{\xi}_{n,2}-\frac{2\rho c^2}{L}\left(\xi_{n,1}-\xi_{n,2}\right)=g\left(\xi_{n+1,1}-\xi_{n,2}\right), \tag{3}$$

where

$$g\left(\Delta\xi\right)=\left(\frac{k_2+k_1}{2}+\frac{k_2-k_1}{2}\operatorname{sign}\left(\Delta\xi\right)\right)\Delta\xi,$$

$\xi_{n,1}$ and $\xi_{n,2}$ denote the displacements of the first and second mass in the discretized model equivalent to the n-th waveguide respectively.

By analyzing the boundary conditions, the following two expressions can be obtained:

$$\rho c\dot{\xi}_0=g\left(\xi_{1,1}-\xi_0\right)-2\rho c^2\xi'_{\rm inc}\left(-ct\right), \tag{4}$$

$$\rho c\dot{\xi}_{N+1}=-g\left(\xi_{N+1}-\xi_{N,2}\right), \tag{5}$$

where ξ_0 denotes the displacement at $x=0$, ξ_{N+1} denotes the displacement at $x=NL$.

We assume that the excitation can be expressed as $\xi_{\rm inc}=A\cos(\omega(x-ct)/c)$, where A, ω, and t are amplitude, angular frequency, and time, then equation (4) can be rewritten as

$$\rho c\dot{\xi}_0=g\left(\xi_{1,1}-\xi_0\right)-2\rho cA\omega\sin\left(\omega t\right). \tag{6}$$

We can obtain the propagation characteristics of fundamental wave and second harmonic wave by solving Eqs. (2), (3), (5), and (6).

2.2. Dispersion curve

We assume that the steady-state solution of the fundamental wave is

$$v_\circ=a_\circ\cos\left(\omega t\right)+b_\circ\sin\left(\omega t\right), \tag{7}$$

then

$$\begin{aligned}\Delta v &= v_\circ-v_\diamond\\ &= \left(a_\circ-a_\diamond\right)\cos\left(\omega t\right)+\left(b_\circ-b_\diamond\right)\sin\left(\omega t\right)\\ &= \sqrt{\left(a_\circ-a_\diamond\right)^2+\left(b_\circ-b_\diamond\right)^2}\sin\left(\omega t+\varphi\right)\\ &= B\sin\left(\omega t+\varphi\right),\end{aligned} \tag{8}$$

where $B=\sqrt{\left(a_\circ-a_\diamond\right)^2+\left(b_\circ-b_\diamond\right)^2}$, $\tan\varphi=\left(a_\circ-a_\diamond\right)/\left(b_\circ-b_\diamond\right)$. Since $B\geq 0$, $\operatorname{sign}\left(\Delta v\right)$ can be simplified as

$$\operatorname{sign}\left(\Delta v\right)=\operatorname{sign}\left(B\sin\left(\omega t+\varphi\right)\right)=\operatorname{sign}\left(\sin\left(\omega t+\varphi\right)\right). \tag{9}$$

Because of the particularity of sign function, it is difficult for us to get the analytical solution. In order to approximate the dispersion curve of the fundamental wave for study, Fourier

expansion is applied on sign function

$$\operatorname{sign}(\sin(\omega t+\varphi))=\sum_{n=0}^{\infty}\frac{4}{\pi(2n+1)}\sin((2n+1)(\omega t+\varphi)). \quad (10)$$

Thus $g(\Delta\nu)$ can be expressed as

$$\begin{aligned}
g(\Delta\nu) &= \left(\frac{k_2+k_1}{2}+\frac{k_2-k_1}{2}\operatorname{sign}(\Delta\nu)\right)\Delta\nu \\
&= \frac{k_2+k_1}{2}\Delta\nu+\frac{k_2-k_1}{2}\operatorname{sign}(\Delta\nu)\Delta\nu \\
&= \frac{k_2+k_1}{2}\left[(a_\circ-a_\diamond)\cos(\omega t)+(b_\circ-b_\diamond)\sin(\omega t)\right] \\
&\quad+\frac{k_2-k_1}{2}\sum_{n=0}^{\infty}\frac{4}{\pi(2n+1)}\sin((2n+1)(\omega t+\varphi)) \\
&\quad\times\left[(a_\circ-a_\diamond)\cos(\omega t)+(b_\circ-b_\diamond)\sin(\omega t)\right] \\
&= \frac{k_2+k_1}{2}\left[(a_\circ-a_\diamond)\cos(\omega t)+(b_\circ-b_\diamond)\sin(\omega t)\right] \\
&\quad+\frac{k_2-k_1}{2}\sum_{n=0}^{\infty}\left\{\frac{2}{\pi(2n+1)}(a_\circ-a_\diamond)\right. \\
&\quad\times\left[\sin((2n+2)\omega t+(2n+1)\varphi)\right. \\
&\quad\left.+\sin(2n\omega t+(2n+1)\varphi)\right] \\
&\quad-\frac{2}{\pi(2n+1)}(b_\circ-b_\diamond) \\
&\quad\times\left[\cos((2n+2)\omega t+(2n+1)\varphi)\right. \\
&\quad\left.\left.-\cos(2n\omega t+(2n+1)\varphi)\right]\right\}. \quad (11)
\end{aligned}$$

It is easy to find that all harmonic components inside the summation notation in Eq. (11) are even harmonics, since we want to study the dispersion curve of fundamental wave, we take

$$\begin{aligned}
g(\Delta\nu) &= \frac{k_2+k_1}{2}\left[(a_\circ-a_\diamond)\cos(\omega t)+(b_\circ-b_\diamond)\sin(\omega t)\right] \\
&= \frac{k_2+k_1}{2}\Delta\nu, \quad (12)
\end{aligned}$$

thus $g(\Delta\xi)$ in Eqs. (2) and (3) can be written as

$$g(\Delta\xi)=\frac{k_2+k_1}{2}\Delta\xi. \quad (13)$$

Substituting Eq. (13) into Eqs. (2) and (3), we obtain

$$\frac{\rho L}{2}\ddot{\xi}_{n,1}+\frac{2\rho c^2}{L}(\xi_{n,1}-\xi_{n,2})=-\frac{k_2+k_1}{2}(\xi_{n,1}-\xi_{n-1,2}), \quad (14)$$

$$\frac{\rho L}{2}\ddot{\xi}_{n,2}-\frac{2\rho c^2}{L}(\xi_{n,1}-\xi_{n,2})=\frac{k_2+k_1}{2}(\xi_{n+1,1}-\xi_{n,2}), \quad (15)$$

According to Bloch's theorem, we assume $\xi_{n,1}=U_1\mathrm{e}^{\mathrm{j}(\omega t-nqL)}$, $\xi_{n,2}=U_2\mathrm{e}^{\mathrm{j}(\omega t-nqL)}$, where U_1 and U_2 denote the displacement amplitudes of the first mass and the second mass in the discretized model equivalent to the n-th waveguide respectively, q denotes wave vector.

By plugging $\xi_{n,1}$ and $\xi_{n,2}$ into Eqs. (14) and (15), we can get

$$\omega=\pm\sqrt{\omega_1^2+\omega_2^2\pm\sqrt{\omega_1^4+\omega_2^4+2\omega_1^2\omega_2^2\cos(qL)}}. \quad (16)$$

where $\omega_1^2=4c^2/L^2$, $\omega_2^2=(k_2+k_1)/\rho L$. According to Eq. (16), we can approximately obtain the dispersion curve of the fundamental wave when BNMU and IMU are arranged periodically.

3. Results

3.1. Results of numerical calculation

We assume that IMU is aluminum, $c=6420$ m/s, $\rho=2700$ kg/m^3, $N=20$ (*i.e.*, the number of BNMU is $N+1=21$), $L=3$ mm, $k_1=3.0k_0$, $k_2=2.4k_0$, the amplitude of the sinusoidal signal is 1 μm (*i.e.*, $A=1$ μm). We use the ode45 algorithm to solve Eqs. (2), (3), (5), and (6) in Subsection 2.1, and obtain the signal received at $x=NL$. The steady-state signal is processed by fast Fourier transform (FFT), then we can obtain the transmission coefficients of the fundamental and the second harmonic waves as shown in Figs. 2(a) and 2(b) respectively.

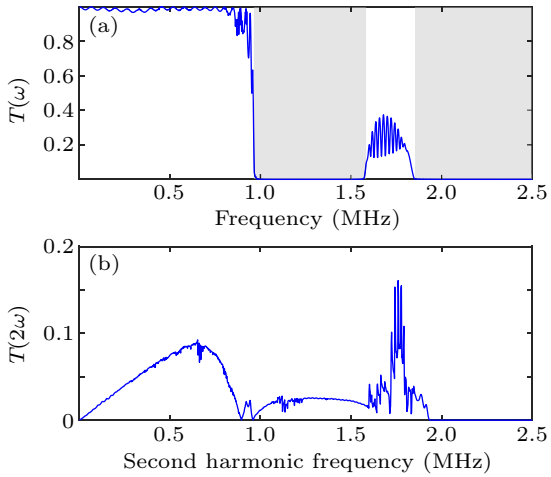


Fig. 2. (a) Transmission coefficient of the fundamental wave as a function of the excitation frequency, and the gray shadows represent the band-gaps calculated by the approximate dispersion relationship of the fundamental wave given in Subsection 2.2. (b) Transmission coefficient of the second harmonic wave as a function of the second harmonic frequency.

We can calculate the location of the band-gap for the fundamental wave by the approximate dispersion relationship of the fundamental wave given in Subsection 2.2, as shown in the shadow part of Fig. 2(a), which is coincident preferably with the result of the numerical calculation in Fig. 2(a).

3.2. Impact of parameters' variation on transmission characteristics

3.2.1. Impact of variation in N

We set N as 3, 8, and 20 respectively, while other parameters are the same as ones in Subsection 3.1. The results are shown in Fig. 3. As N increases, for fundamental wave, the transition between pass-band and band-gap becomes sharper, and the band-gap becomes more evident; as for the second harmonic wave, its transmission coefficient is improved in some frequency bands, since the nonlinear effect is enhanced with

the increase of N, which means in order to give full play to the performance of the system in practical application, it would be better to select larger N value. Therefore, we choose $N = 20$ in our model.

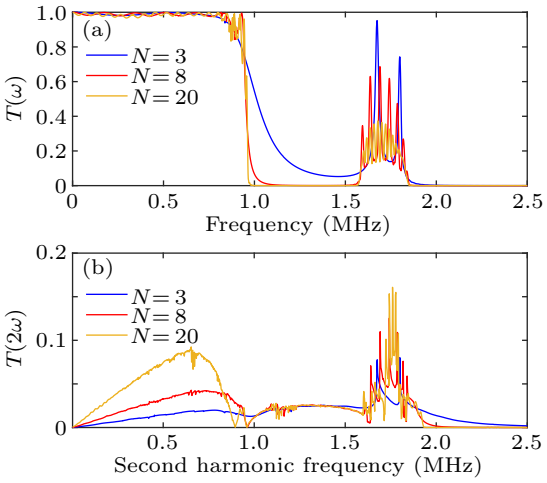


Fig. 3. (a) Transmission coefficient of the fundamental wave as a function of the excitation frequency. (b) Transmission coefficient of the second harmonic wave as a function of the second harmonic frequency.

3.2.2. Variation of nonlinear spring's stiffness

(i) Impact of variation in k_1.

We set k_1 as $2.5k_0$, $3.0k_0$, and $3.3k_0$ respectively, while other parameters are the same as ones in Subsection 3.1. The results are shown in Fig. 4. Figure 4(b) shows the transmission coefficient of the fundamental wave, which indicates that with the increase of k_1, the acoustic branch of the fundamental wave does not move, while the optical branch moves towards the high frequency range. Figure 4(a) shows the dispersion curve of the fundamental wave calculated by the method in Subsection 2.2, which well explains the movement of fundamental wave's optical branch. Figure 4(c) shows the transmission coefficient of second harmonic wave, which indicates that with the increase of k_1, the second pass-band of the second harmonic wave moves towards the high frequency range, and the transmission coefficient of the second pass-band becomes higher. As for the reason, it is easy to know by Eq. (1) that the strength of nonlinearity is proportional to the gap between k_1 and k_2, and here $k_2 = 2.4k_0$, so the gap between k_1 and k_2 gradually widens as k_1 changes from $2.5k_0$ to $3.3k_0$, resulting in the increase of second pass-band's transmission coefficient.

(ii) Impact of variation in k_2.

We set k_2 as $2.3k_0$, $2.4k_0$, and $2.7k_0$ respectively, while other parameters are the same as ones in Subsection 3.1. The results are shown in Fig. 5. Figure 5(b) shows the transmission coefficient of the fundamental wave, which indicates that with the increase of k_2, the acoustic branch of the fundamental wave does not move, while the optical branch moves towards the high frequency range. Figure 5(a) shows the dispersion curve of the fundamental wave calculated by the method in Subsection 2.2, which well explains the movement of fundamental wave's optical branch. Figure 5(c) shows the transmission coefficient of the second harmonic wave, which indicates that with the increase of k_2, the second pass-band of the second harmonic wave moves towards the high frequency range, and the transmission coefficient of the second pass-band becomes lower, since the strength of nonlinearity is proportional to the gap between k_1 and k_2, and here $k_1 = 3.0k_0$, so the gap between k_1 and k_2 gradually decreases as k_2 changes from $2.3k_0$ to $2.7k_0$, resulting in the decrease of second pass-band's transmission coefficient.

From above results it can be found that the band-gap and the amplitude of the second harmonic wave can be manipulated by changing the stiffness of nonlinear spring.

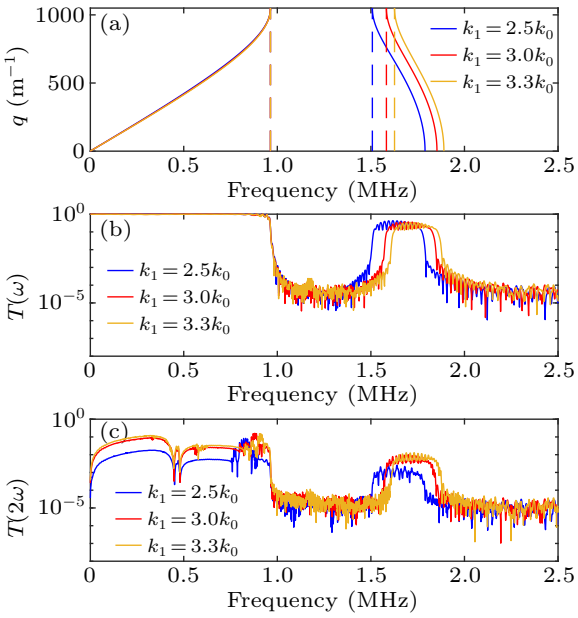


Fig. 4. (a) Dispersion curve of the fundamental wave calculated approximately. (b) Transmission coefficient of the fundamental wave as a function of the excitation frequency. (c) Transmission coefficient of the second harmonic wave as a function of the excitation frequency.

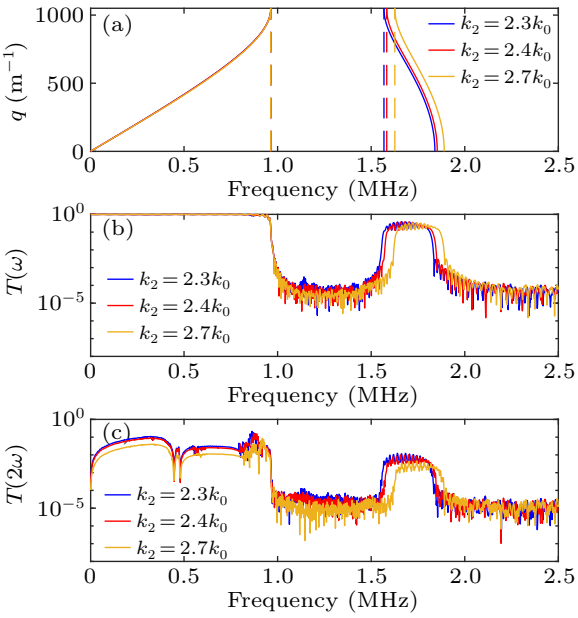


Fig. 5. (a) Dispersion curve of the fundamental wave calculated approximately. (b) Transmission coefficient of fundamental wave as a function of the excitation frequency. (c) Transmission coefficient of the second harmonic wave as a function of the excitation frequency.

3.2.3. Variation of L between adjacent BNMUs

We set L as 2.7 mm, 3.0 mm, and 3.5 mm respectively, while other parameters are the same as ones in Subsection 3.1. The results are shown in Fig. 6. Figure 6(a) shows the dispersion curve of the fundamental wave calculated by the method in Subsection 2.2. In Fig. 6(b), with the increase of L, the acoustic and optical branch of the fundamental wave both move towards the low frequency range, which is consistent with the movement of dispersion curve in Fig. 6(a). Figure 6(c) shows the transmission coefficient of the second harmonic wave, which indicates that with the increase of L, the first and the second pass-bands of the second harmonic wave move towards the low frequency range. In other words, the band-gap can be adjusted by changing L between adjacent BNMUs.

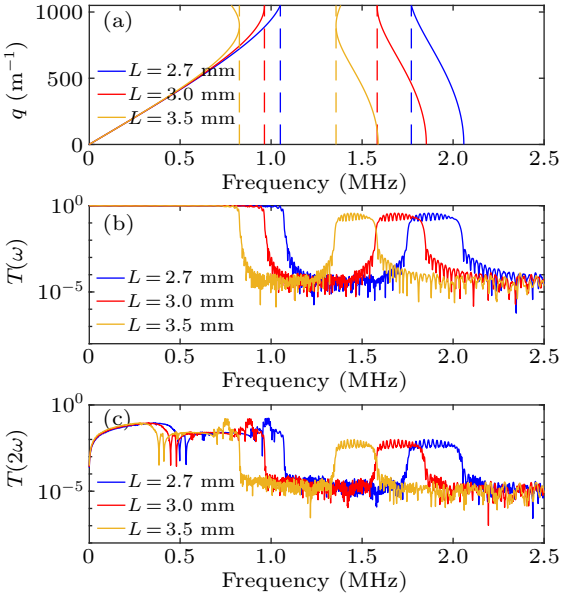


Fig. 6. (a) Dispersion curve of the fundamental wave calculated approximately. (b) Transmission coefficient of the fundamental wave as a function of the excitation frequency. (c) Transmission coefficient of the second harmonic wave as a function of the excitation frequency.

3.3. Partially periodic arrangement of BNMU

In this section, we assume that cells of BNMU and IMU arranged alternately (for simplicity, the cell consisting of a BNMU and an IMU is denoted as ψ_1) only occupy part of the waveguide we wish to study, and the rest is occupied by another kind of cell, which is the result of substituting BNMU with IMU2 (IMU2 is another isotropy material unit, whose stiffness is equal to k_1). In other words, the rest of the waveguide is occupied by cells of IMU2 and IMU arranged alternately (for simplicity, the cell consisting of an IMU2 and an IMU is denoted as ψ_2). The total number of BNMU and IMU2 is still set as $N+1=21$, the frequency of the excitation signal is 0.7 MHz, while other parameters are the same as ones in Subsection 3.1. For simplicity, we denote the position of the i-th BNMU or IMU2 as R_i.

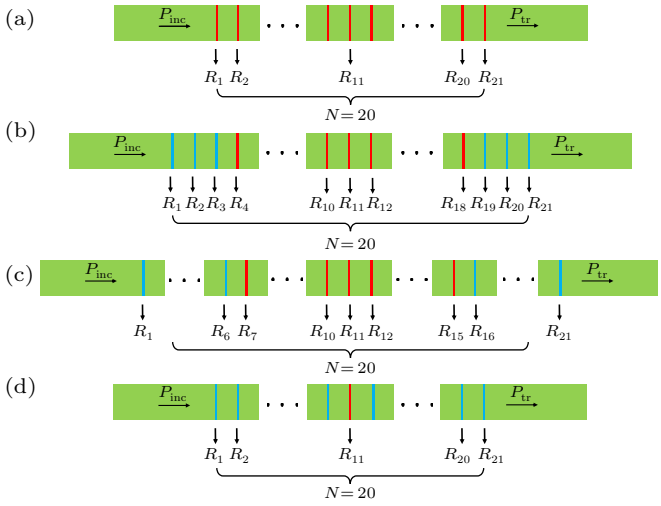


Fig. 7. (a) Schematic diagram of periodic arrangement of BNMU and IMU. (b) Schematic diagram of the case when there are 15 ψ_1 (ψ_1 denotes the cell of BNMU and IMU arranged alternately) in the waveguide and the rest are ψ_2 (ψ_2 denotes the cell of IMU2 and IMU arranged alternately), the red part is BNMU, the blue part is IMU2, and the rest is IMU. (c) Schematic diagram of the case when there are 9 ψ_1 in the waveguide and the rest are ψ_2, the red part is BNMU, the blue part is IMU2, and the rest is IMU. (d) Schematic diagram of the case when there is only one ψ_1 in the waveguide and the rest are ψ_2, the red part is BNMU, the blue part is IMU2, and the rest is IMU.

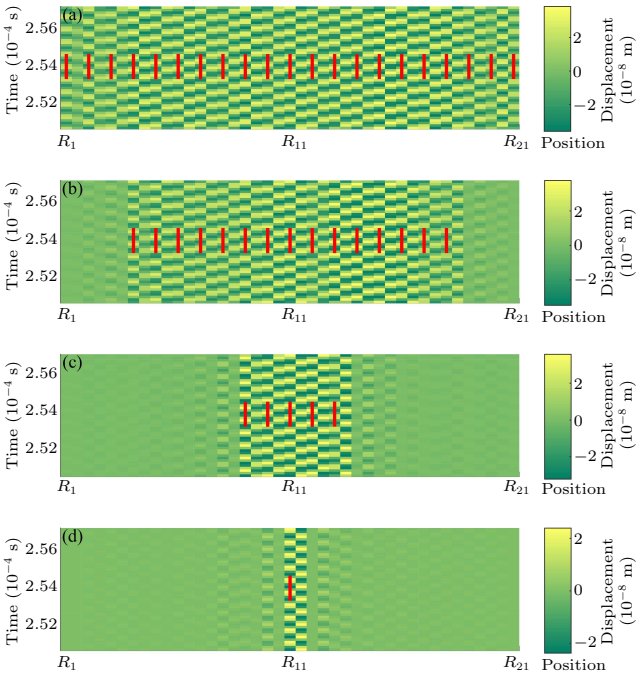


Fig. 8. (a) The second harmonic wave propagation result of Fig. 7(a) when excitation frequency is 0.7 MHz. (b) The second harmonic wave propagation result of Fig. 7(b) when excitation frequency is 0.7 MHz. (c) The second harmonic wave propagation result of Fig. 7(c) when excitation frequency is 0.7 MHz. (d) The second harmonic wave propagation result of Fig. 7(d) when excitation frequency is 0.7 MHz.

On the basis that the excitation signal is sinusoidal signal, we study three cases: the first one is that there is only one ψ_1 and the rest is occupied by ψ_2, the second one is that there are 9 ψ_1 and the rest is occupied by ψ_2, the last one is that there are 15 ψ_1 and the rest is occupied by ψ_2, furthermore, we compare these three cases with the case when BNMU and IMU are

arranged periodically, the schematic diagram of the cases we describe above are shown in Fig.7, corresponding results are shown in Fig. 8.

Figures 8(a)–8(d) show the second harmonic wave propagation results when excitation frequency is 0.7 MHz, the abscissa represents the position of the i-th BNMU or IMU2 (*i.e.*, R_i), and the ordinate represents the time. Figure 8(a) shows the result of periodic arrangement of BNMU and IMU strictly, in which the second harmonic wave can completely propagate to the end of the waveguide. Figures 8(b) and 8(c) show the second harmonic wave propagation results of Figs. 7(b) and 7(c), respectively, it can be seen that the propagation of the second harmonic wave to the end of the waveguide is hindered by reducing the number of ψ_1. Figure 8(d) shows the second harmonic wave propagation result of Fig. 7(d), it can be seen that when the number of ψ_1 reduces to one, the second harmonic wave can hardly be received at the end of the waveguide.

As for the reason why the phenomenon we describe above exists, we think it is because the second harmonic wave (corresponding frequency is 1.4 MHz) generated by exciting a sinusoidal signal of 0.7 MHz is in the pass-band for the case in which BNMU and IMU are arranged periodically (corresponding transmission coefficient of second harmonic wave is shown in Fig. 9(e), the red dotted line is at 1.4 MHz), while 1.4 MHz is in the band-gap for the case in which IMU2 and IMU are arranged periodically (corresponding transmission coefficient of fundamental wave is shown in Fig. 9(d), the red dotted line is at 1.4 MHz). Furthermore, for 0.54 MHz–0.77 MHz, second harmonic wave is in the pass-band when BNMU and IMU are arranged periodically, while it is in the band-gap when there is only one ψ_1 (*i.e.*, the number of BNMU is only one). As the number of ψ_1 increases (*i.e.*, the number of BNMU increases), the second harmonic wave is hindered less, and the conversion degree of band-gap to pass-band is deepened, which represents as the transmission coefficient of the second harmonic wave increases and becomes closer to the one when BNMU and IMU are arranged periodically, as shown in the green box in Figs. 9(a)–9(c). Therefore, for the second harmonic wave, the conversion of pass-band and band-gap can be realized at specific frequency band by nonlinear metamaterial.

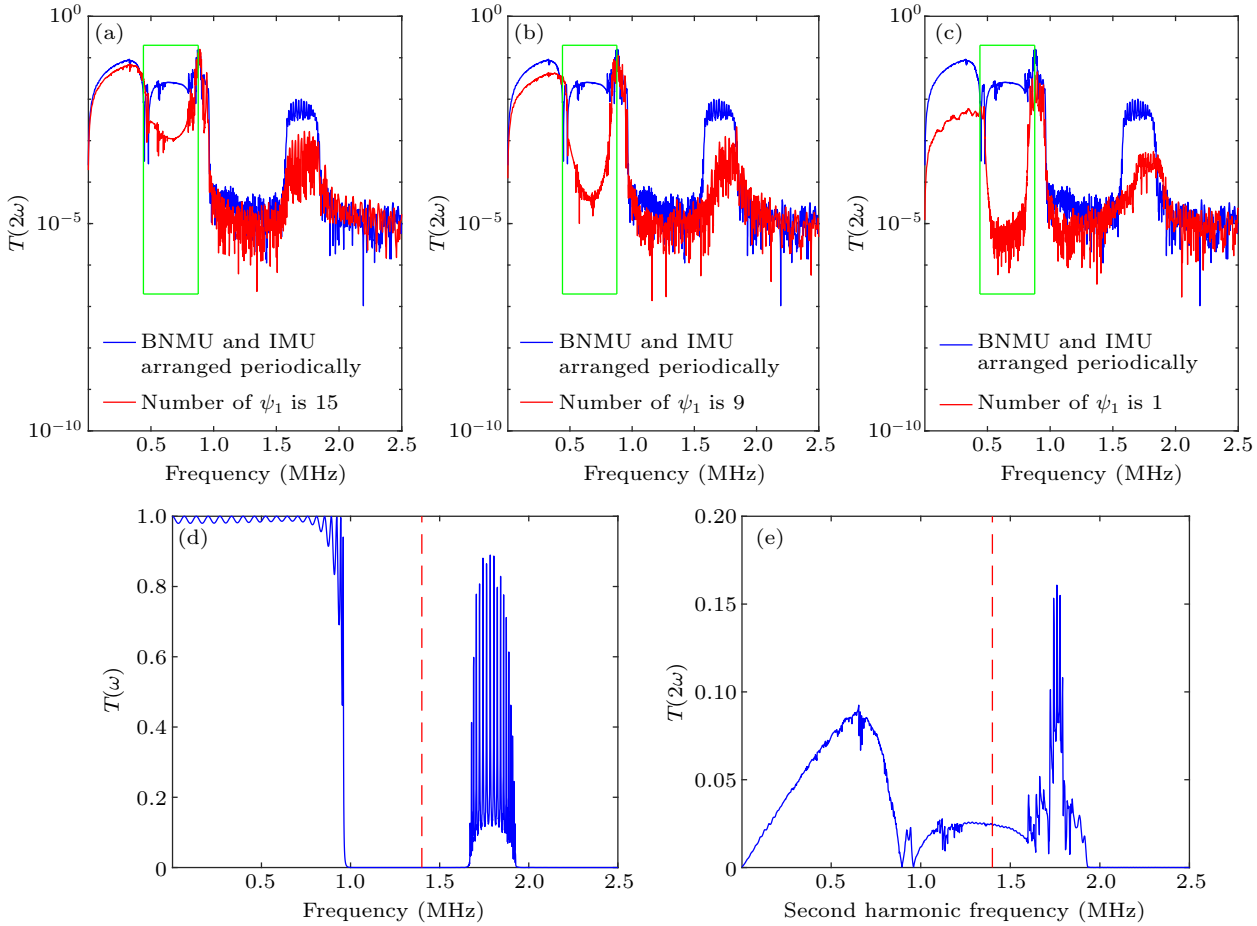


Fig. 9. (a) Transmission coefficient of the second harmonic wave as a function of the excitation frequency when there are $15\psi_1$ (*i.e.*, number of BNMU is 15) and BNMU and IMU are arranged periodically. (b) Transmission coefficient of the second harmonic wave as a function of the excitation frequency when there are $9\psi_1$ (*i.e.*, number of BNMU is 9) and BNMU and IMU are arranged periodically. (c) Transmission coefficient of the second harmonic wave as a function of the excitation frequency when there is one ψ_1 (*i.e.*, number of BNMU is one) and BNMU and IMU are arranged periodically. (d) Transmission coefficient of the fundamental wave when IMU2 and IMU are arranged periodically. (e) Transmission coefficient of the second harmonic wave when BNMU and IMU are arranged periodically.

4. Conclusion

In this work, we have studied the propagation of nonlinear sound waves in 1D chain of masses connected by nonlinear springs with bilinear property. We discretized the 1D chain with periodic arrangement of nonlinear units with bilinear property to establish the mass-linear/nonlinear spring models, and derived the corresponding equations of motion and boundary conditions, according to which we can obtain the numerical solution of nonlinear acoustic wave propagation. Furthermore, we applied the Fourier expansion on the sign function to obtain approximate dispersion curve of the fundamental wave, which can predict the location of band-gap.

Through the method above, we have obtained the propagation characteristics of the fundamental and the second harmonic waves. At the same time, we have also studied the influence of parameters' variation on the transmission characteristics of the fundamental and second harmonic waves. We find the band-gap can be manipulated by changing the stiffness of nonlinear material units with bilinear property and the distance between them. Moreover, we have investigated the case of partially periodic arrangement of BNMU, and find that it is possible to convert the pass-band and band-gap into each other at specific frequency bands.

Different from the traditional researches on nonlinear acoustic metamaterials, the source of nonlinearity that we apply in this paper is bilinear nonlinearity. The results of nonlinear metamaterials revealed here can be used to manipulate the band-gap of nonlinear metamaterials, and the results of partially periodic (or 'defective') nonlinear metamaterials can be used to study the conversion between pass-band and band-gap for the second harmonic wave, both of them can be beneficial for the research of nonlinear acoustics.

Acknowledgments

Project supported by the National Key Research and Development program of China (Grant No. 2020YFA0211400), the State Key Program of the National Natural Science of China (Grant No. 11834008), the National Natural Science Foundation of China (Grant No. 12174192), the Fund from the State Key Laboratory of Acoustics, Chinese Academy of Sciences (Grant No. SKLA202008), and the Fund from the Key Laboratory of Underwater Acoustic Environment, Chinese Academy of Sciences (Grant No. SSHJ-KFKT-1701).

References

[1] Liu Z Y, Zhang X X, Mao Y W, Zhu Y Y, Yang Z Y, Chan C T and Sheng P 2000 *Science* **289** 1734
[2] Yang Z, Mei J, Yang M, Chan N H and Sheng P 2008 *Phys. Rev. Lett.* **101** 204301
[3] Mei J, Ma G, Yang M, Yang Z Y, Wen W J and Sheng P 2012 *Nat. Commun.* **3** 756
[4] Li J and Chan C T 2004 *Phys. Rev. E* **70** 055602
[5] Feng L, Liu X P, Chen Y B, Huang Z P, Mao Y W, Chen Y F, Zi J and Zhu Y Y 2005 *Phys. Rev. B* **72** 033108
[6] Seo Y M, Park J J, Lee S H, Park C M, Kim C K and Lee S H 2012 *J. Appl. Phys.* **111** 023504
[7] Yang M, Ma G C, Yang Z Y and Sheng P 2013 *Phys. Rev. Lett.* **110** 134301
[8] Alagoz S, Alagoz B B, Sahin A and Nur S 2015 *Chin. Phys. B* **24** 046201
[9] Ke M Z, Liu Z Y, Cheng Z G, Li J, Peng P and Shi J 2007 *Solid State Commun.* **142** 177
[10] Li J, Fok L, Yin X B, Bartal G and Zhang X 2009 *Nat. Mater.* **8** 931
[11] Jia H, Ke M Z, Hao R, Ye Y T, Liu F M and Liu Z Y 2010 *Appl. Phys. Lett.* **97** 173507
[12] Yang X S, Yin J, Yu G K, Peng L H and Wang N 2015 *Appl. Phys. Lett.* **107** 193505
[13] Zhu X F, Liang B, Kan W W, Zou X Y and Cheng J C 2011 *Phys. Rev. Lett.* **106** 014301
[14] Li T H, Huang M, Yang J J, Lan Y Z and Sun J 2012 *J. Vib. Acoust.* **134** 051016
[15] Li B L, Li T H, Wu J, Hui M, Yuan G and Zhu Y S 2017 *Acoust. Phys.* **63** 45
[16] Cai C, Yuan Y, Kan W W, Yang J and Zou X Y 2016 *Chin. Phys. B* **25** 124302
[17] Ren C Y, Xiang Z H and Cen Z Z 2011 *Chin. Phys. B* **20** 114301
[18] Liang B, Guo X S, Tu J, Zhang D and Cheng J C 2010 *Nat. Mater.* **9** 989
[19] Fang X, Wen J H, Bonello B, Yin J F and Yu D L 2017 *Nat. Commun.* **8** 1288
[20] Guo X X, Gusev V E, Bertoldi K and Tournat V 2018 *J. Appl. Phys.* **123** 124901
[21] Kulkarni P P and Manimala J M 2019 *Acta Mechanica* **230** 2521
[22] Grinberg I and Matlack K H 2020 *Wave Motion* **93** 102466
[23] Golub M V, Doroshenko O V, Fomenko S I, Wang Y Z and Zhang C Z 2021 *International Journal of Solids and Structures* **212** 1
[24] Jeon G J and Oh J H 2021 *Phys. Rev. E* **103** 012212
[25] Dutta D, Sohn H, Harries K A and Rizzo P 2009 *Structural Health Monitoring* **8** 251